International Journal of Chemical and Biochemical Sciences
(ISSN 2226-9614)

Journal Home page: www.iscientific.org/Journal.html

A new classification based on Keros classification to assess the olfactory fossa depth variations using CBCT (Retrospective study)

Wessam Mohamed Magdy Aly Youssef [1], Mo'men Ali Ameen Hamela[2], Dalia Ali Abou-Alnour [3]*

[1*]*Researcher-Surgery and Oral medicine department, Oral and Dental research institute, National Research Center, Egypt*

[2]*Lecturer of otolaryngology, Faculty of Medicine, Cairo University, Egypt*

[3]*Lecturer, oral and maxillofacial radiology, Faculty of Oral and dental medicine, Modern University for technology and information (MTI), Egypt*

Abstract

This study aimed to assess the olfactory fossa depth variations using CBCT through a new classification based on Keros classification. A sample of 100 CBCT maxillofacial scans were retrospectively retrieved from a NewTom GIANO HR 3D CBCT machine. A new hybrid classification was associated with gender, age, and depth of the right and left sides of the olfactory fossae. In the right side, comparison between different classes among male and female revealed insignificant difference as P=0.95. In the left side, comparison between different classes among male and female revealed significant difference as P=0.02, which demonstrated significant association between gender and Keros classification of the left side. Regarding the New Hybrid Classification, comparison between different classes among male and female revealed significant difference as P=0.04, which demonstrated significant association between gender and specific classes (in class III male revealed 87.5%, while female revealed 12.5 %/ in class VI male revealed 80% and female revealed 20% / in class IX male revealed 0%, and female revealed 100%). The current study findings lead us to advocate cone beam computed tomography in Endoscopic sinus surgery for the examination of the olfactory fossae. According to the classic keros classification type II olfactory fossae were the most common type. While, the new hybrid classification concluded that asymmetry in the olfactory fossa depth was seen in 21% of the overall cases, where class IV was the most dominant.

Keywords: Olfactory fossa depth, Keros classification, Endoscopic sinus surgery, Cone-Beam CT.

Full length article **Corresponding Author*, e-mail: wessam2004@gmail.com

1. Introduction

Endoscopic sinus surgery (ESS) is an often-recommended procedure that can be used to treat a wide range of conditions, including mucocele, optic nerve compression, sellar and parasellar tumours, and nasal polyposis [1]. However, this procedure has both minor and significant side effects, including bleeding, tooth or lip numbness, infections, ostial stenosis, extra-ocular muscle injury, and infections [1]. A depression in the anterior cranial cavity is called the olfactory fossa (OF). Its floor is the cribriform plate (CP) of the ethmoid. The nasal cavity and the anterior cerebral fossa are divided by this fine bony plate. Crista galli and the lateral lamella of the cribriform plate (LLCP) are, respectively, the lateral and medial constraints of olfactory fossa [2]. The fovea ethmoidalis, a portion of the frontal bone that divides the ethmoidal cells from the front cerebral fossa, is where LLCP travels vertically and meets superolaterally [3]. The fovea ethmoidalis and lateral lamella are the most significant sections of the skull base in terms of the risk of complication development during ESS because the lateral lamella is the thinnest and most fragile bone of the skull base [4-5]. The depth of the olfactory fossa is used to measure the height of the lateral lamella (Keros classification). Keros divided the depth of the olfactory fossae into three categories in 1962: type I (less than 3 mm), type II (4–7 mm), and type III (8–16 mm) [6]. Keros type III is the most vulnerable, given that LLCP poses a significant risk of iatrogenic harm [7].

The gold standard in the presurgical examination of the PNS has been thought to be radiographic study utilizing multidetector computed tomography (MDCT), which offers an understanding of the anatomic variances of the ethmoid roof in every patient. Due to its low radiation dose and high-resolution pictures, cone beam computed tomography (CBCT) is commonly utilized in dentistry and otorhinolaryngology for the examination of PNS [8]. Asymmetry in the depth or height of the olfactory fossa (OF) is associated with a higher risk of cerebral penetration during procedures like ESS and CBCT radiation dose is significantly lower than that of MDCT, so in the current study we engender a new classification based on Keros classification to assess the variations between right and left olfactory fossa depth of the same patient using CBCT [8-9].

2. Methods

A sample of 100 CBCT maxillofacial scans (50 males and 50 females) of mean age 31.15 for males and 34.36 for females, were retrospectively retrieved from database of NewTom GIANO HR 3D CBCT machine with FSV: 3.00 mA, 90 kV, FOV: [16 × 18e], exposure time 7.2s at the department of oral and maxillofacial radiology, faculty of dentistry. The study is approved by the research ethics committee, Faculty of dentistry, with reference REC-D 838-3. The study is performed by two maxillofacial radiologists with more than 10 years of experience. Sample size was calculated using EPI INFO version 7.2.5.0, according to the results of a previous study in which the prevalence of asymmetry (difference between the two sides < 0.01 mm) was (93%)- by adopting a confidence interval of (95%), a margin of error of (5%) with finite population correction [10].

2.1. Inclusion criteria

The inclusion criteria consisted of scans of patients with completely developed PNS, acquired for any reason (i.e., implant treatment planning, impacted teeth, orthodontic treatment planning, etc.) showing the crista galli of the ethmoidal bone and nasal fossa, with no gender consideration.

2.2. Exclusion criteria

Excluded criteria consisted of patients with a history of paranasal sinus surgery, maxillofacial trauma, pathological processes in the PNS, low-quality images, images containing only lower jaw, and images containing artifacts, which made visualization of anatomical structures difficult.

2.3. Radiographic assessment

All of the CBCT scans were evaluated using The Medical Imaging Interaction Toolkit (MITK-v2022.10) software as the anterior ethmoidal artery is transmitted through the anterior ethmoidal sinus/complex via the anterior ethmoidal canal (foramen), entering the olfactory fossae via the point at which the frontal bone connects to the LLCP; we considered the anterior ethmoidal foramen as a reference for the superior limit measurement of the olfactory fossa height [11]. On the coronal view, first of all we centralized the crosshair on the anterior ethmoidal foramen of the evaluated side (right or left), and then we drown circle centralized on the crosshair using the Measurement sub bottom of the Quantification bottom. This was how the superior border of the olfactory fossa was determined (Figure 1). Using the sagittal view, we evaluated the CP searching for the deepest point, then the second step was the centralization of the crosshair on the CP deepest point of the same side also on the coronal view. This was how the inferior border of the olfactory fossa was determined. Then, we dragged the edge of the drown circle in the first step to flush with the crosshair centralized on the CP deepest point, so the radius of the drown circle determined the height of the olfactory fossa depth (Figure 2). We classified the evaluated right and left olfactory fossa depth separately first based on the traditional Keros classification, and then for the same patient olfactory fossa depth assigned a new classification (New Hybrid Classification) as follow:

I. Both right and left olfactory fossae are 1-3 mm deep.
II. Both right and left olfactory fossae are 4-7 mm deep.
III. Both right and left olfactory fossae are 8-16 mm deep.
IV. Asymmetrical OF depth (class I Rt with class II Lt).
V. Asymmetrical OF depth (class I Rt with class III Lt).
VI. Asymmetrical OF depth (class II Rt with class III Lt).
VII. Asymmetrical OF depth (class I Lt with class II Rt).
VIII. Asymmetrical OF depth (class I Lt with class III Rt).
IX. Asymmetrical OF depth (class II Lt with class III Rt).

25% of the images were revaluated by the both radiologists at one week interval and the inter and intra-observer reliability has been calculated.

2.4. Statistical analysis

Statistical analysis was performed with SPSS 16 ® (Statistical Package for Scientific Studies), Graph pad prism & windows excel.

3. Results

All quantitative data were presented as mean &standard deviation, while qualitative data were presented as frequency and percentages. Exploration of the given quantitative data was performed using Shapiro-Wilk test and Kolmogorov-Smirnov test for normality which revealed that the significant level (P-value) was insignificant as P-value > 0.05 which indicated that all data originated from normal distribution (parametric data) resembling normal Bell curve. CBCT maxillofacial scans of 100 adult patients (50 males and 50 females) were evaluated for the assessment of olfactory fossa depth. In males the age was 31.15±11.03, while in females the age was 34.36±11. Inter and intra-observer reliability were measured by Inter Class Correlation coefficient, which shown excellent reliability in all measurements as ICC >0.75 (Table 1).

3.1. Distribution of gender, right side Keros classification, left side Keros classification, and the New Hybrid Classification

Distribution of gender, right side classification, left side classification, and the New Hybrid Classification among studied samples were presented in Table 2.

- In the right side, there was a significant difference between classes. Class II (73%) was significantly the highest, then class III (14%), while class I (13%) was significantly the lowest, as P<0.0001.
- In the left side, there was a significant difference between classes Class II (78%) was significantly the highest, then class III (13%), while class I (9%) was significantly the lowest, as P<0.0001.
- Regarding the New Hybrid Classification, there was a significant difference between classes, Class II (65%) was significantly the highest, while class VII (3%) was significantly the lowest. On the other hand, there was no cases revealed class V & VIII (0%) as P<0.0001.

3.2. Description of age, right side depth, and left side depth

Minimum, maximum, mean and standard deviation of age, right side depth in mm, and left side depth mm were presented in **Table 3**.

- Regarding the age, male (31.15±11.03) was significantly lower than female (34.36±11) as P=0.003.
- Regarding the depth in mm, right side (5.48 ± 1.77) was insignificantly higher than left side (5.35±1.69).

3.3. Distribution of different Keros classes among gender regarding Right side, left side and the New Hybrid Classification

Distribution of different classes among gender regarding Right side, left side and the New Hybrid Classification, and comparison between them using Chi square test were presented in Table 4.

- In the right side, comparison between different classes among male and female revealed insignificant difference as P=0.95.
- In the left side, comparison between different classes among male and female revealed significant difference as P=0.02, which demonstrated significant association between gender and Keros classification of the left side (in class III male revealed 84.6%, while female revealed 15.4%).
- Regarding the New Hybrid Classification, comparison between different classes among male and female revealed significant difference as P=0.04, which demonstrated significant association between gender and specific classes (in class III male revealed 87.5%, while female revealed 12.5% / in class VI male revealed 80% and female revealed 20% / in class IX male revealed 0%, and female revealed 100%).

3.4. Right and left sides depth (mm) among different gender

Mean and standard deviation of right and left depth (mm) in both male and female were presented in Table 5.

- In right side, male (5.63 ± 1.75) was insignificantly higher than female (5.32 ± 1.79), with 0.3 mean difference, and P=0.39.
- In left side, male (5.67 ± 1.88) was insignificantly higher than female (5.03 ± 1.42), with 0.64 mean difference, and P=0.06.

3.5. Distribution of different olfactory fossae olfactory fossae depth categories

The olfactory fossae in the overall sample were categorized according to the depth in mm among males and females into four categories (< 1 mm, 1-2 mm, 2-3 mm and >3 mm) Table 6. Comparison between male and female revealed insignificant difference as P=0.34.

4. Discussion

Chronic rhinosinusitis is the first and most typical ESS indication [12]. The floor of the olfactory fossa, a depression in the anterior cranial cavity, is made up of the ethmoid's cribriform plate [13]. Olfactory fossa depth is categorized by the Keros classification; the deeper the olfactory fossa is (higher Keros type), the greater the danger of skull base injury. The lateral lamella and cribriform plate are the most often injured areas [12]. Only five research have used CBCT to date (Bayrak et al., 2020, Sancar and Duman 2022, Mahdian et al., 2022, Güldner et al., 2012, and Costa et al., 2019) [8,14-17]. Many studies have evaluated the olfactory fossa utilizing MDCT. Whereas the research conducted by Sancar and Duman in 2022, evaluated the relationship between olfactory fossa depth and hypoplastic maxillary sinuses and the research conducted by Güldner et al., in 2012 analyzed the anterior skull base relevant structures with a focus on age-dependent differences which is unrelated to the case selection and the goals of the current study [15-16]. Functional endoscopic sinus surgery causes more damage when the fossa is deep or asymmetrical since the depth of the olfactory fossa differs between patients' sides [12-13]. Therefore, in the current study, we created a new classification (New Hybrid Classification), which was modified from Keros one to classify the depth of olfactory fossa from I to IX classes while specifically taking into account the likely changes between the right and left sides. In the current study; there was a significant difference between classes distribution (I-IX) based on the New Hybrid Classification (P<0.0001). Olfactory fossa depth of most cases was type II (65%) followed by type III (8%) then type IV (7%), meaning that most cases was Keros type II (both right and left sides) which matches the results of the previous studies and regarding the current study if asymmetry exist it will be Keros class IV (I Rt with class II Lt) (Table 2) [8,13-14,18-20]. Based on the New Hybrid Classification, asymmetry in the OF depth was seen in 21% of the overall cases (7% IV, 5% VI, 3% VII and 6% IX), where asymmetry was slightly higher in females than males (10% males and 11% females) (Table 2). Prior investigations by Bayrak et al., (2020) and Mahdian M. et al., (2022) revealed asymmetry between the right and left sides of 24.88% and 33.3%, respectively in studies carried out utilizing MDCT, Abdullah B. et al., (2020), Babu et al., (2018), Adeel et al., (2013), and Alazzawi et al., (2012) reported asymmetry of 26%, 75%, 94.8%, and 95%, respectively [8,10,13-14,21-22].

This wide range of asymmetrical olfactory fossa depth between the right and left sides may be caused by differences in how asymmetry is judged and expressed in mm. According to Abdullah et al., (2020), asymmetry was reported when the right-left difference was >3 mm, whereas according to Alazzawi et al., (2012), asymmetry was supposed when the difference between the two sides was 0.01 mm [10,21]. This wide range of asymmetrical olfactory fossa depth between the right and left sides may be caused by differences in how asymmetry is judged and expressed in mm. Any instance that had distinct right and left keros classifications was recognized in the current analysis as an asymmetrical case. Male and female distribution of the New Hybrid Classification showed a significant difference with a P=0.04 (Table 4). Class IX (class II Lt with class III Rt) showed a strong correlation with females (100%), while class III (class III for both Rt & Lt sides) & VI (class II Rt with class III Lt) showed a considerable association with men (87.5% & 80%, respectively). According to the data, males have deeper left than right olfactory fossa, whereas females have deeper right than left Olfactory fossa. Traditional Keros classes I, II, and III were distributed as 11%, 72.5%, and 13.5% in the current study, indicating that class II was the most prevalent. which was comparable to earlier CBCT investigations by Mahdian et al., (2022) [8] and Costa et al., (2019), where Keros class II was 65,52% and 66.26%, respectively [8,17]. The present investigation revealed that distribution for Keros class III was higher than for class I. In contrast to Mahdian et al., (2022), who reported Keros distribution as 20.43% and 13.31% for class I and III, respectively, Costa et al., (2019), found that Keros class I and III were 13.79% and 20.69%, respectively [8,17]. This can be as a result of the fact that the aforementioned researches were conducted on various demographics. The current investigation demonstrated a significant difference in the left-side Keros classification distribution between males and females as P=0.02 (Table 4), where class III in males revealed 84.6% while females revealed 15.4%.

Costa et al., (2019) and Bayrak et al., (2020) reported no significant difference in the Keros classification among different gender or sides, whereas Mahdian et al., (2022) reported a significant difference among right and left sides, which may be explained by the different age range and sample size used [8,14,17]. As shown in Table 3, the difference between the right and left olfactory fossa heights in the current study (p=0.21) was not statistically significant (5.48mm 1.77 and 5.35mm 1.69, respectively). According to CT studies by Alazzawi et al. (2012), Souza et al., (2008), and Lebowitz et al., (2001), olfactory fossa depth was higher in the left than the right side, contradicting the findings of our study and others, which may be because of racial or sample size variations [7,10,23-27]. Males and females measured 5.63mm 1.75 mm and 5.32mm 1.79 mm in height on the right side, respectively, while males and females measured 5.67mm 1.88 mm and 5.03mm 1.42 mm on the left side, indicating that olfactory fossa is marginally deeper in males than in females (Table 5). The current study results correlate with Tawfik et al., (2022), who reported that the height of right and left olfactory fossa in males and females was (Rt: 4.88mm±0.73 vs. 4.72mm±0.65; Lt: 4.81mm±0.71 vs. 4.69 mm±0.64, respectively) and Bayrak et al., (2020) who reported that olfactory fossa height was (Rt: 4.5mm±2.21 vs. 4.49mm±2.07; Lt: 4.37mm±1.67 vs. 4.11 mm±1.63) for males and females respectively [14,20]. In the present investigation, the difference between the right and left sides was less than 1 mm in 79% of cases and between 1 and 2 mm in 13% of instances (Table 6). In 95% of cases, according to Alazzawi et al., (2012), the difference between the sides was less than 2 mm, while in 5% of cases, it was between 2-4 mm [10]. Babu et al., (2018) indicated that, similar to the findings of the current study, the majority of cases exhibited a discrepancy between the two sides of 1 mm (64.6%) [13]. Comparatively, Abdullah et al., (2020) stated that 26% of cases showed difference in sides height >3mm [21]. In our investigation, only 2% of cases showed difference >3mm.

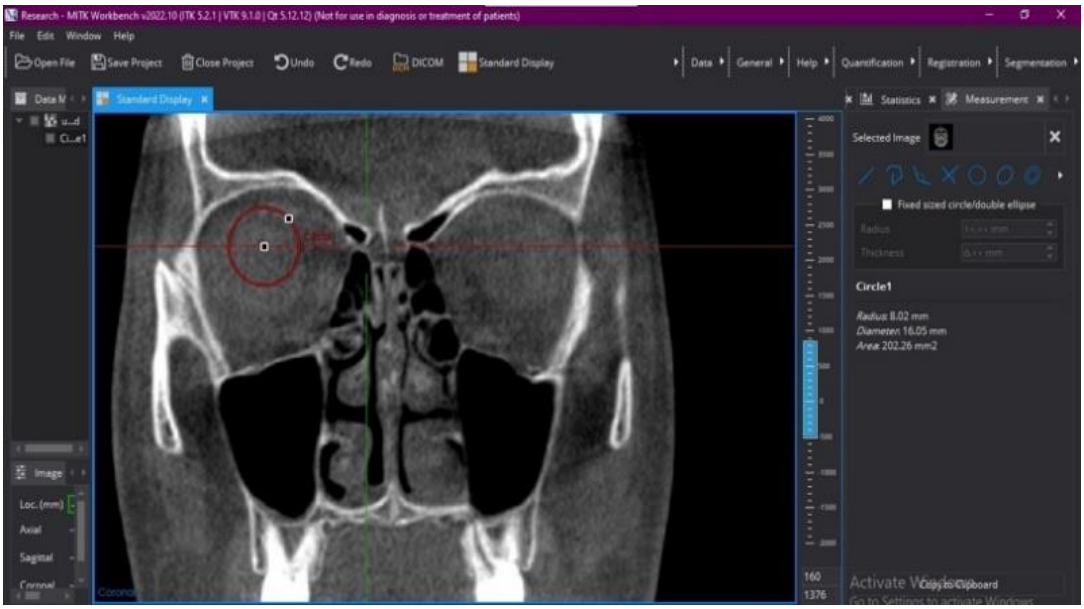

Figure 1: MITK viewer showing coronal CBCT cut where the crosshair is centralized on the right anterior ethmoidal foramen to determine the superior border of the olfactory fossa depth using the center of a drown measurement circle as a reference.

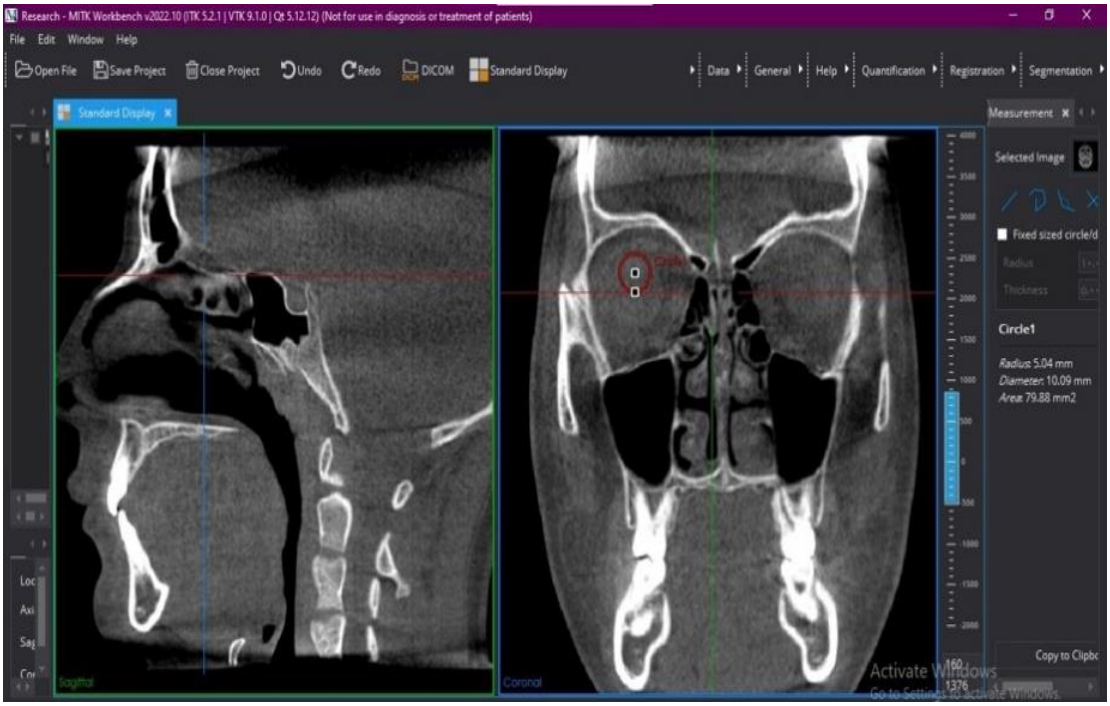

Figure 2: MITK viewer showing the centralization of the crosshair on the cribriform plate deepest point on sagittal view (left), where the inferior border of the olfactory fossa was determined. The edge of the drown measurement circle is flush with the crosshair centralized on the cribriform plate deepest point in the coronal view (right).

Table 1: Intra-observer reliability and interobserver reliability.

		ICC	95% CI		P value
			L	U	
Intra-observer reliability	**Rt Depth in mm**	0.991	0.980	0.996	0.0001**
	RT Class	1.000	1.000	1.000	----
	Lt Depth in mm	0.990	0.978	0.996	0.0001**
	Lt Class	1.000	1.000	1.000	----
	New Hybrid Classification no.	1.000	1.000	1.000	-----
Interobserver reliability	**Rt Depth in mm**	0.998	1.00	1.00	0.00
	RT Class	1.000	1.00	1.00	-----
	Lt Depth in mm	0.997	0.99	1.00	0.00
	Lt Class	1.000	1.00	1.00	-----
	New Hybrid Classification no.	1.000	1.00	1.00	-----

ICC: Intraclass Correlation, CI: confidence interval, L: lower arm, U: upper arm, **Highly Significant as P<0.001.

Table 2: Gender, Right side Keros classification, and left side Keros classification, and the New Hybrid Classification among studied cases.

		N	%	P value
Gender	Male	50	50.0%	1.00 ns
	Female	50	50.0%	
Keros Classification	Class I	22	11%	<0.0001*
	Class II	151	75.5%	
	Class III	27	13.5%	
Right side Keros classification	Class I	13	13.0%	<0.0001**
	Class II	73	73.0%	
	Class III	14	14.0%	
Left side Keros classification	Class I	9	9.0%	<0.0001**
	Class II	78	78.0%	
	Class III	13	13.0%	
New Hybrid Classification	Class I	6	6.0%	<0.0001**
	Class II	65	65.0%	
	Class III	8	8.0%	
	Class IV	7	7.0%	
	Class V	0	0.0%	
	Class VI	5	5.0%	
	Class VII	3	3.0%	
	Class VIII	0	0.0%	
	Class IX	6	6.0%	

N: frequency, %: percentages, Ns: non-significant difference as P>0.05, **Highly Significant difference as P<0.001.

Table 3: Minimum, maximum, mean and standard deviation of age, right, and left depth in mm.

		Minimum	Maximum	Mean	Standard Deviation	P value
Age	**Male**	18	61	31.15	11.03	0.003**
	Female	18	59	34.36	11.00	
	Overall	18	61	27.94	10.17	
Right Depth in mm		1.99	10.25	5.48	1.77	0.21 ns
Left Depth in mm		1.45	10.06	5.35	1.69	

Ns: non-significant difference as P>0.05, **Highly significant difference as P<0.001.

Table 4: Distribution of different Keros classes among gender regarding Right and left sides, the New Hybrid Classification and comparison between them using Chi square test.

		Total	Gender				Chi-square	P value
			Male		Female			
			N	%	N	%		
Right side Keros classification	Class I	13	7	53.8%	6	46.2%	0.09	0.95
	Class II	73	36	49.3%	37	50.7%		
	Class III	14	7	50.0%	7	50.0%		
Left side Keros classification	Class I	9	5	55.6%	4	44.4%	7.62	0.02*
	Class II	78	34	43.6%	44	56.4%		
	Class III	13	11	84.6%	2	15.4%		
New Hybrid Classification	Class I	6	3	50.0%	3	50.0%	6.1	0.04*
	Class II	65	30	46.2%	35	53.8%		
	Class III	8	7	87.5%	1	12.5%		
	Class IV	7	4	57.1%	3	42.9%		
	Class V	0	0	0.0%	0	0.0%		
	Class VI	5	4	80.0%	1	20.0%		
	Class VII	3	2	66.7%	1	33.3%		
	Class VIII	0	0	0.0%	0	0%		
	Class IX	6	0	0.0%	6	100.0%		

N: frequency, %: percentages, Ns: non-significant difference as P>0.05, * Significant difference as P<0.05.

Table 5: Mean and standard deviation of right and left sides depth in mm in male and female, and comparison between them using Paired t test.

Depth in mm	Gender				Difference (Independent t test)				
	Male		Female		MD	SED	95% CI		P value
	M	SD	M	SD			L	U	
Right side	5.63	1.75	5.32	1.79	0.30	0.35	-0.40	1.01	0.38 ns
Left side	5.67	1.88	5.03	1.42	0.64	0.33	-0.02	1.30	0.06 ns

M: mean, SD: standard deviation, MD: mean difference, SED: standard error difference, CI: confidence interval, L: lower arm U: upper arm, Ns: non-significant difference as P>0.05.

Table 6: Olfactory fossa depth categories in the overall sample among males and females, and comparison between them using Chi square test.

	Overall		Male		Female		Chi square	P value
	N	%	N	%	N	%		
< 1 mm	79	79.0%	41	51.9%	38	48.1%	3.5%	0.34
1-2 mm	13	13.0%	5	38.5%	8	61.5%		
2-3 mm	6	6.0%	4	66.7%	2	33.3%		
>3 mm	2	2.0%	0	0.0%	2	100.0%		

N: frequency, %: percentages, Ns: non-significant difference as P>0.05.

5. Conclusions

The findings of this study advocate cone beam computed tomography for the examination of the olfactory fossae. This research also concluded that according to the classic keros classification type II olfactory fossae were the most common type. While, the new hybrid classification taken in this study concluded that asymmetry in the depth of the olfactory fossae was seen in 21% of the overall cases (7% IV, 5% VI, 3% VII and 6% IX), where asymmetry was slightly higher in females than males.

References

[1] K. C. McMains. (2008). Safety in endoscopic sinus surgery. Current Opinion in Otolaryngology & Head and Neck Surgery. 16 (3): e247-e251.

[2] T. G. Jacob, J. M. Kaul. (2014). Morphology of the olfactory fossa–A new look. Journal of the anatomical society of India. 63 (1): e30-e35.

[3] H. R. Stammberger, D. W. Kennedy. (1995). Paranasal sinuses: anatomic terminology and nomenclature. Annals of Otology, Rhinology & Laryngology. 104 (10): e7-e16.

[4] J. Kainz, H. Stammberger. (1988). The roof of the anterior ethmoid: a locus minoris resistentiae in the skull base. Laryngologie, Rhinologie, Otologie. 67 (4): e142-e149.

[5] T. Ohnishi, T. Tachibana, Y. Kaneko, S. Esaki. (1993). High-risk areas in endoscopic sinus surgery and prevention of complications. The Laryngoscope. 103 (10): e1181-e1185.

[6] P. Keros. (1962). On the practical value of differences in the level of the lamina cribrosa of the ethmoid. Zeitschrift fur Laryngologie, Rhinologie, Otologie und ihre Grenzgebiete. 41 (1): e809-e813.

[7] S. A. Souza, M. M. A. D. Souza, M. Idagawa, Â. M. B. Wolosker, S. A. Ajzen. (2008). Computed tomography assessment of the ethmoid roof: a relevant region at risk in endoscopic sinus surgery. Radiologia Brasileira. 41 (1): e143-e147.

[8] M. Mahdian, M. Karbasi Kheir. (2022). CBCT assessment of ethmoid roof variations through Keros, Gera, and TMS classifications. International Journal of Otolaryngology.

[9] C. Nardi, C. Talamonti, S. Pallotta, P. Saletti, L. Calistri, C. Cordopatri, S. Colagrande. (2017). Head and neck effective dose and quantitative assessment of image quality: a study to compare cone beam CT and multislice spiral CT. Dentomaxillofacial Radiology. 46 (7).

[10] S. Alazzawi, R. Omar, K. Rahmat, K. Alli. (2012). Radiological analysis of the ethmoid roof in the Malaysian population. Auris Nasus Larynx. 39 (4): e393-e396.

[11] L. Naidu, L. A. Sibiya, O. S. Aladeyelu, C. O. Rennie. (2023). Anatomical landmarks for localisation of the anterior ethmoidal artery: a combined radiological and cadaveric (endoscopic) study. Surgical and Radiologic Anatomy. 45 (5): e545-e554.

[12] M. T. Homsi, M. M. Gaffey. (2020). Sinus endoscopic surgery.

[13] A. C. Babu, M. R. P. B. Nair, A. M. Kuriakose. (2018). Olfactory fossa depth: CT analysis of 1200 patients. Indian Journal of Radiology and Imaging. 28 (4): e395-e400.

[14] S. Bayrak, C. A. Belgin, K. Orhan. (2020). Evaluation of the relationship between olfactory fossa measurements and nasal septum deviation for endoscopic sinus surgery. Journal of Craniofacial Surgery. 31 (3): e801-e803.

[15] B. Sancar, S. B. Duman. (2022). Olfactory Fossa Evaluation as a Maxillary Sinus Development Using Cone Beam Computed Tomography. Indian Journal of Otolaryngology and Head & Neck Surgery. 74 (2): e1566-e1570.

[16] C. Güldner, A. P. Zimmermann, I. Diogo, J. A. Werner, A. Teymoortash. (2012). Age-dependent differences of the anterior skull base. International journal of pediatric otorhinolaryngology. 76 (6): e822-e828.

[17] A. L. F. Costa, A. K. Paixão, B. C. Gonçalves, C. M. Ogawa, T. Martinelli, F. A. Maeda, T. Trivino, S. L. P. D. C. Lopes. (2019). Cone beam computed tomography-based anatomical assessment of the olfactory fossa. International journal of dentistry.

[18] H. Kaplanoglu, V. Kaplanoglu, A. Dilli, U. Toprak, B. Hekimoğlu. (2013). An analysis of the anatomic

variations of the paranasal sinuses and ethmoid roof using computed tomography. The Eurasian journal of medicine. 45 (2): e115.

[19] Z. A. Almushayti, A. N. Almutairi, M. A. Almushayti, H. S. Alzeadi, E. A. Alfadhel, A. N. AlSamani, A. Almutairi, M. Almushayti, E. A. Alfadhel Sr. (2022). Evaluation of the Keros classification of olfactory fossa by CT scan in Qassim region. Cureus. 14 (2).

[20] A. E. TAWFIK, H. M. SHERIEF, F. ZIDAN. (2022). Radiographic Analysis of Ethmoid Roof Based on KEROS Classification among Egyptian People Using Multidector CT: A Cross-Sectional Study. The Medical Journal of Cairo University. 90 (9): e1499-e1504.

[21] B. Abdullah, S. C. Chew, M. E. Aziz, N. M. Shukri, S. Husain, S. W. Joshua, D. Y. Wang, K. Snidvongs. (2020). A new radiological classification for the risk assessment of anterior skull base injury in endoscopic sinus surgery. Scientific reports. 10 (1): e4600.

[22] M. Adeel, M. Ikram, M. S. A. Rajput, A. Arain, Y. J. Khattak. (2013). Asymmetry of lateral lamella of the cribriform plate: a software-based analysis of coronal computed tomography and its clinical relevance in endoscopic sinus surgery. Surgical and radiologic anatomy. 35 (1): e843-e847.

[23] L. Shapiro. (2001). Computer vision.:/shapiro l., stockman G. Prentence Hall.

[24] R. A. Alrumaih, M. M. Ashoor, A. A. Obidan, K. M. Al-Khater, S. A. Al-Jubran. (2016). Radiological sinonasal anatomy: exploring the saudi population. Saudi Medical Journal. 37 (5): e521.

[25] B. Santosh. (2017). A study of clinical significance of the depth of olfactory fossa in patients undergoing endoscopic sinus surgery. Indian Journal of Otolaryngology and Head & Neck Surgery. 69 (4): e514-e522.

[26] C. A. Solares, W. T. Lee, P. S. Batra, M. J. Citardi. (2008). Lateral lamella of the cribriform plate: software-enabled computed tomographic analysis and its clinical relevance in skull base surgery. Archives of Otolaryngology–Head & Neck Surgery. 134 (3): e285-e289.

[27] M. Bista, M. Maharjan, P. Kafle, S. Shrestha, T. Kc. (2010). Computed tomographic assessment of lateral lamella of cribriform plate and comparison of depth of olfactory fossa.